DOI: https://doi.org/10.46632/mc/1/2/9

Materials and its Characterization
Vol: 1(2), 2022
REST Publisher; ISBN: 978-81-948459-0-4
Website: http://restpublisher.com/book-series/materials-and-its-characterization/

Mechanical Properties of NiTi Based Shape Memory Alloy used in Manufacturing of Mars Rover Wheels: Short Review

Unnati Parmar, * Ankit Kumar Mishra
Astroex Research Association, Deoria, Uttar Pradesh, India
*Corresponding author Email**:** ankitkumarm1998@gmail.com

Abstract. Shape memory alloys (SMA) are innovatively designed for engineering applications including, but not limited to, medical devices, actuators, micromechanical systems, deployable structures, and elastocaloric devices. Prior to the manufacture of any component for the above mentioned applications, an extensive simulation study is recommended as the basic properties are required to be filled in the software. The unavailability of to-the-point literature makes this task difficult for researches. In this paper, an overview of binary NiTi based shape memory alloy is given, where its characteristic physical properties i.e. shape memory effect and super elastic effect, and mechanical properties like fatigue failure, stress-strain characteristics and yield and ultimate strength is stated for several different specimens prepared using thermomechanical methods.
Keywords: Application, Mars Rover, Properties, Shape Memory Alloys.

1. Introduction

Shape memory alloys (SMA) are, to this day, the most important shape memory materials which come under the category of smart materials whose properties can be manipulated by external means according to their applications and mission specifications. Nickel and titanium based memory alloys are developed as binary NiTi and TiTa, ternary NiTiW, NiTiCu, TiTaHf, TiVAl, TiNiZr, TiNiFe, CuAlNi and quaternary TiVAlY, TiVAlB, TiVAlCo, TiVAlCu, CuAlNiHf, CuAlNiMn, CuAlNiGd, CuAlNiCo, CuZnAlZr, CuZnAlTi shape memory alloys. [17] The binary NiTi alloy is often preferred in engineering applications because of its excellent functional performance and biocompatibility. Thanks to the phase transformations (i.e. B2 → R/B2 → B19′) occurred in NiTi alloys which are responsible for exhibiting both shape memory effect and superelasticity. The aforementioned phase transformation depends on their composition and the thermo-mechanical treatment. [18] The main problem of NiTi parts production is the manufacturing costs. Current trends in the manufacturing processes focus on reduction of material waste, together with an increase in production efficiency, which leads to the emergence of new technological processes. One of such a new family of methods is additive manufacturing (AM). [19] The two major popularly utilized aspects of the functional behavior of NiTi alloys are the shape memory effect (SME) and superelasticity (SE). SME is commonly used in actuators and deployable structures, while SE has wider application fields, the most popular ones being medical stents and elastocaloric cooling systems. [20] The spring tyre model for upcoming Mars Rover missions also utilize the superelastic effect (SE), in order to withstand greater deformations caused by some of the rougher exploration sites on martian terrain such as the one encountered by Curiosity rover.

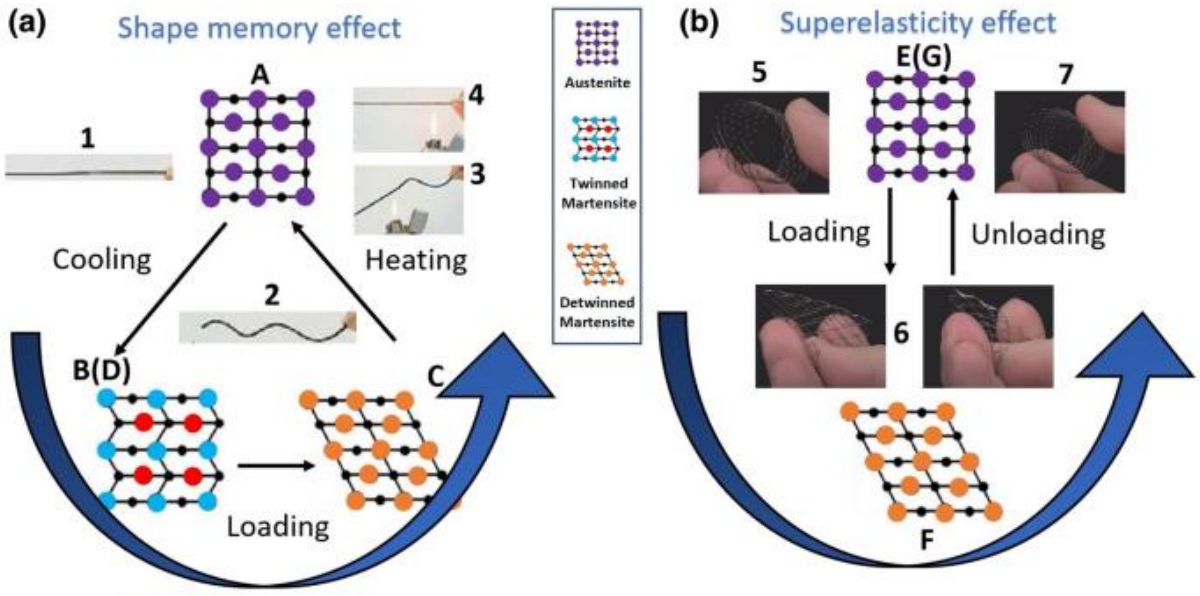

FIGURE 1. Phase transformations exhibited by NiTi memory alloy under SME and SE [21]

K. Garg et al (2022) describes the development of smart materials from traditional composites and investigates the three factors: stress, strain and temperature which determine the nature of material and the fact that manipulating these factors by a combination of thermomechanical processes allowed shape memory alloys to perform their characteristics more efficiently; characters such shape memory effect, superelasticity, hysteresis, high damping effect, etc. Also, the applications of SMAs corresponding to each of these properties were studied [1]. Jinguo Ge et al (2022) studied the micro-hardness mapping which indicated that homogenous anti-indentation properties were acquired regardless of location variations [2]. To highlight the effect of Ni, Guangfeng Shi et al (2022) studied Ni-rich NiTi alloys with different building orientations of 0◦, 45◦ and 90◦ fabricated by LPBF to conclude that during the friction process, sample 90◦ was more favorable for the formation of tribo-layers since the [111] orientation is characterized as "hard" and was attributed to a combined action of the highest nano hardness, and highest critical stress for the stress-induced martensitic transformation [3]. K. Xu et al. (2022) utilizes isothermal compression followed by aging to design R and B2 nano-domains, and super elastic instability for as deformed NiTi and superelastic stability for as-aged NiTi. Results showed that SIMT occurs during first loading for as-deformed and as aged NiTi. Since crystalline structures of B_2 and R phase are similar, a three-step shear mode for SIMT is proposed for as-deformed and as-aged NiTi, which could decrease atomic shear displacement while meet the requirement of stacking order [4]. Saint-Sulpice et al. (2022) studies the fatigue life of shape memory alloys from the help of mean endurance limit and SNP curves and shows the benefits of this method that are it only need one sample and results can be obtained in a few hours of tests and processing of data [5].

Now, to signify the effects of environmental conditions on the surface of shape memory alloy, firstly Z. Zhu et al. (2022) studied the effect of hydrogen by performing cathodic hydrogen charging for the wires at a current density of $10A/m^2$ with various charging times (2.5min, 5min, 7.5min and 10min) and charging lengths (2 cm, 4 cm, 6 cm and 8 cm) at room temperature [6]. H. Vashishtha et al (2022) with the help of XPS and Raman spectrum assessment emphasized the formation of TiO2 and NiO passive film after exposure to saline water solution. A shattered valley-type structure confirmed the film breakdown, and elemental mapping validated the Ni2+ dissolution from the test surface [7]. G. Shi et al. (2022) successfully investigated the MTTs of SLM-fabricated NiTi alloys using response surface methodology. The accuracy of the model was verified by comparing the model predictions with the experimental data to further show that MTTs was affected by the interaction of laser power and scanning speed. [8] G. Liu et al. (2022) studied cold metal transfer (CMT) -fabricated NiTi alloys and it illustrated the fact that the micro-hardness, critical stress, and elongation of CMT-fabricated NiTi alloys increase monotonously from 256 to 290 HV, from 483 to 643 MPa and from 6.39% to 6.75%, respectively [9]. G. Crowther et al (2021) investigated a series of tensegrital wheels which showed that maintaining a class 1 tensegrity as much as possible improves force diffusion and general compliance and also that for high-tension tensegrity, positively constraining tendons at each node is critical to limit unintentional shifting of components, and to prevent parts from shaking loose from high-frequency vibrations [10]. J. Chen, Z. Wang, S. Wang et al. (2022) prepared the HfH_2-decorated NiTi powder by mixing the HfH2 powder with near-equiatomic NiTi powder under high-purity grade argon and studied its mechanical and functional properties along with martensitic phase transformation [11]. Bhattarai et al (2021) gave a brief of The Lunar Roving Vehicle's (LRV) wheel used in the manned Apollo-17 mission, the Lunokhod-1 wheel used in the robotic Luna-17 mission, and a new design called the Tweel design to be used for future NASA missions [12]. X. Dong et al. (2021) studied the uniaxial tensile testing and water bath heating on TiO2 films with thicknesses of approximately 100 and 50 nm which were deposited on dumbbell-shaped plate samples of an NiTi shape memory alloy [13]. A. Bhardwaj et al. (2021) performed constrained groove pressing in order to modify the strength and ductility of NiTi sheet and yield strength, ultimate tensile strength, microhardness and uniform elongation were found to be improved in all the constrained groove pressing'ed and constrained groove pressing aged specimens [14]. X. Wang et al. (2021) studied an anomalous phenomenon on two loading cycles of NiTi shape memory alloys when deforming at the temperature close to the border of superelastic window to show that critical stress for inducing martensite transformation during the second loading cycle is higher than that of the first cycle. Also, the plateau stress of the second cycle decreases to the original level when the strain overcomes the limit of the first cycle. [15]. K. Mehrabi et al. (2012) showed one-way shape memory effect (OWSME) by bending of a ribbon NiTi specimen and room temperature tensile test; and two-way shape memory effect (TWSME) by tensile and bending training. It was seen that NiTi25Cu ribbons exhibit better repeatability and stability during thermal cycles than NiTi ribbons, which show irreversible stresses. [16]

2. Overview on Shape Memory Alloys

Smart materials are those which can be designed by significantly modifying one or more properties through means of external stimuli. Shape memory alloys (SMAs) belong to this family because of their two remarkable characteristics, namely, shape memory effect (SME) and superelastic effect (SE), and have been innovatively employed in various fields, such as sensors, actuators, robotics, aerospace, civil engineering, and medicine. [22] The shape memory and superelastic effects are originated from the thermoelastic martensitic transformation (MT), which is nothing but the ability of shape memory alloys (SMAs) to undergo reversible martensitic phase transformations on application of heating or cooling within specific temperature ranges. [23]. Buehler and Wiley discovered a nickel-titanium alloy in 1961 called nitinol that exhibited a much greater SME than previous materials. This material was a binary alloy of nickel and titanium in a ratio of 55% to 45%, respectively. A 100% recovery of strain up to a maximum of about 8% pre-strain was achieved in this alloy. Another interesting feature noticed was a more than 200% increase in Young's modulus in the high-temperature phase compared to the low-temperature phase. [24] The high temperature phase is the austenite phase which is can bear a much greater deal of stress than the low temperature martensite phase. Temperature plays an important role in the thermomechanical behavior of NiTi shape

memory alloys. In general, the characteristic phase transformation temperatures consist of four types: martensite start temperature (M_s), martensite finish temperature (M_f), austenite start temperature (A_s), and austenite finish temperature (A_f). B2 austenite phase is stable when the temperature is greater than A_f, or between A_f and A_s. [25] NiTi based shape memory alloys exhibit two major phases- martensite phase and austenite phase. Shape memory effect (SME) Memory alloys, when at lower temperatures, exist in martensite phase. At this phase, they bear to be easily deformed when under external stress application. This obviously means that their shape has been changed and is usually seen at temperatures below martensitic finish temperature (M_f). Now, when the memory alloy is heated up to austenite finish temperatures (A_f) and above, they "remember" their shape before deformation. This phenomenon is termed as shape memory effect (SME). The martensitic phase transformation is a first order displacive process in which generally a body centered cubic parent phase, also called austenite phase (A), transforms by mainly a shearing mechanism in a martensite phase (M), which is less ordered than the mother phase [5]. **Super elastic effect (SE)** Super elasticity is the property where a material can undergo large amounts of deformation and still possess the capability to return to their shape before deformation upon removal of the external stress. For example, when a cylindrical element of memory alloy is taken, it exists at martensite phase. Now when it is made to bend in half (at room temperature), it will induce a phase change to austenite at the location of bend. But since austenite is unstable at lower temperatures, it will revert back to its original shape when the external stress is removed. NiTi based shape memory alloys (nitinol) can deform 10–30 times as much as ordinary metals and return to their original shape.

3. Mechanical properties of NiTi based Shape Memory Alloys

Fatigue and fracture **Fatigue life:** The mean fatigue life study of NiTi based shape memory alloy was estimated using self-heating test. Self-heating test involves employing a series of successive steps with incremental maximum stress values (σ_{max} is lower than the transformation yield stress, σ_0, of the material); each step consisted of bloc of sinusoidal cycles between the minimum stress, σ_{min} = 10 MPa, and a given maximum stress for a second at a frequency of 30 Hz, followed by a pause of 100s. From the curve obtained, it is seen that the last three points [fig.2] show a linear regression and the straight line intersecting from maximum stress axis gives the corresponding mean fatigue life. But to obtain a reference limit for the self-heating test, classical high cycle fatigue test was also carried out. The respective SN curves are plotted below [fig.3&4], where the dashed green lines represent the least squares fitting of a Stromeyer-like fatigue law: $\sigma = kNp + \Sigma\, f\ at\ \infty$ ..... (1) and the dashed red lines, the corresponding mean fatigue limit, $\Sigma\, f\ at\ \infty$. The comparison of the two results is given by Table 1. [5]

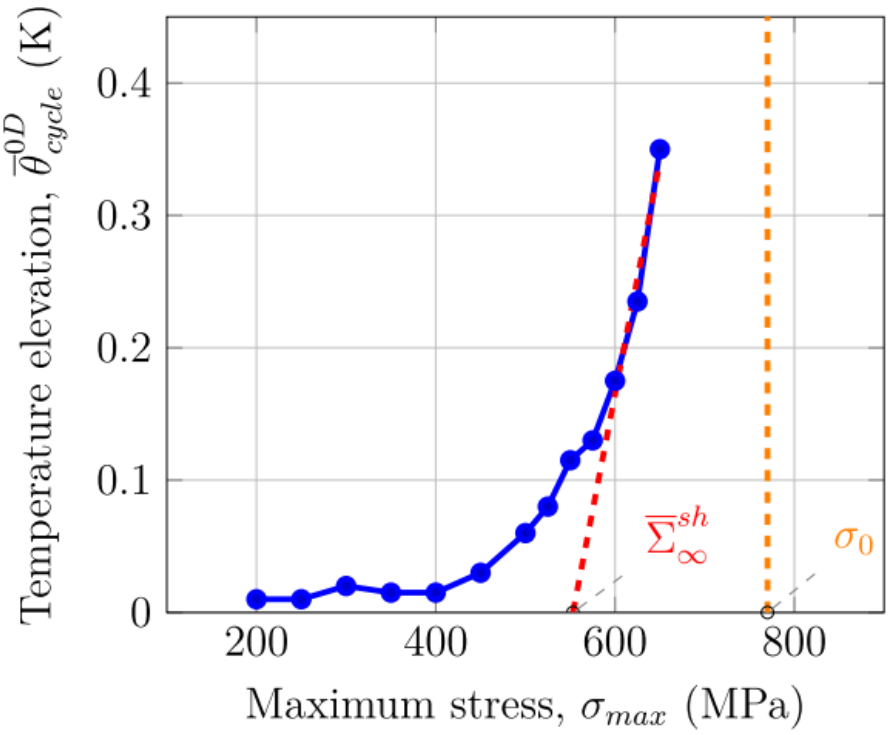

FIGURE 2. Temperature elevation versus maximum stress, with empirical determination of mean endurance limit on specimen [5]

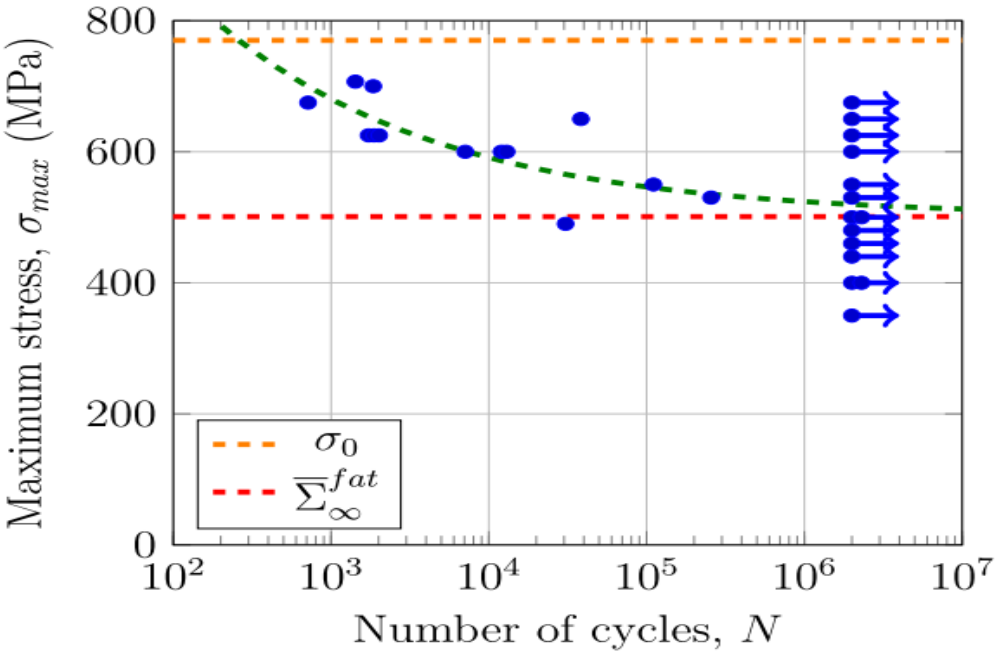

FIGURE 3. Maximum stress versus number of cycles to failure [5]

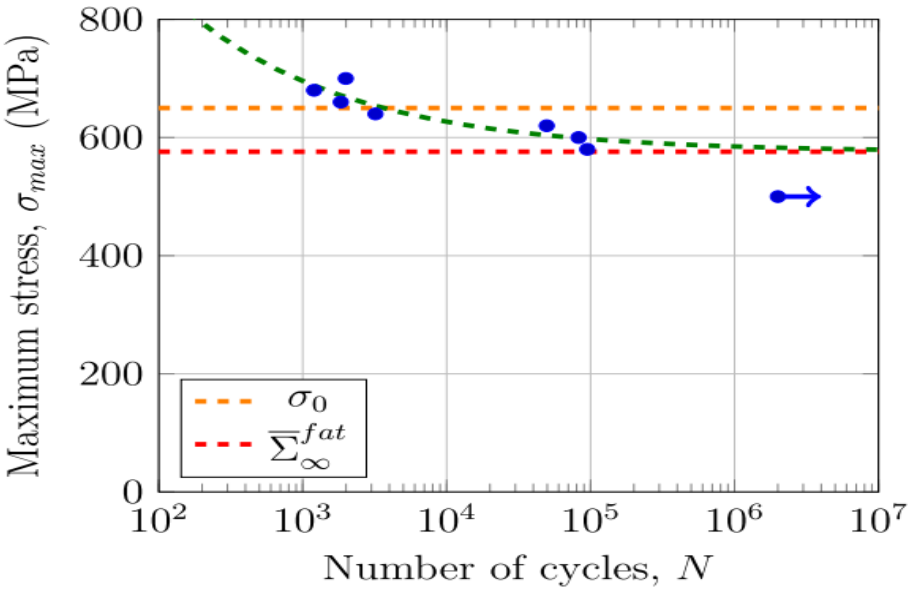

FIGURE 4. Maximum stress versus number of cycles to failure [5]

TABLE 1. Comparison of mean fatigue limit,

Specimen	A (MPa)	B (MPa)	C (%)
d10	501	552	10.2
d12	576	544	-5.56

Table 1. Comparison of mean fatigue limit, where column A gives mean fatigue limit with classic fatigue tests and column B gives mean fatigue limit with self-heating procedure under cyclic loading [5] As the case was for steel, we are seeing agreement in the values for endurance limit given by both the experiments. [5] **Fracture:** Two NiTi SMAs with 50.3 at.% Ni (martensitic/pseudoplastic at room temperature) and 50.7 at.% Ni (austenitic/pseudoelastic at room temperature). At 2000 N, a small subcrack at approximately 45° to the main crack grows upward. At 2700 N, it has become the dominant crack, leaving the old crack tip (marked by white arrows pointing to the upper right in the last two micrographs in Fig. 4a) 15 µm behind. Similarly, a microscopic crack extension is observed for the pseudoelastic NiTi at loads of 2750 and 3500 N. As illustrated by white arrows pointing up in Fig. 4(b), the distance of the crack tip from a ledge increases by 5 µm.

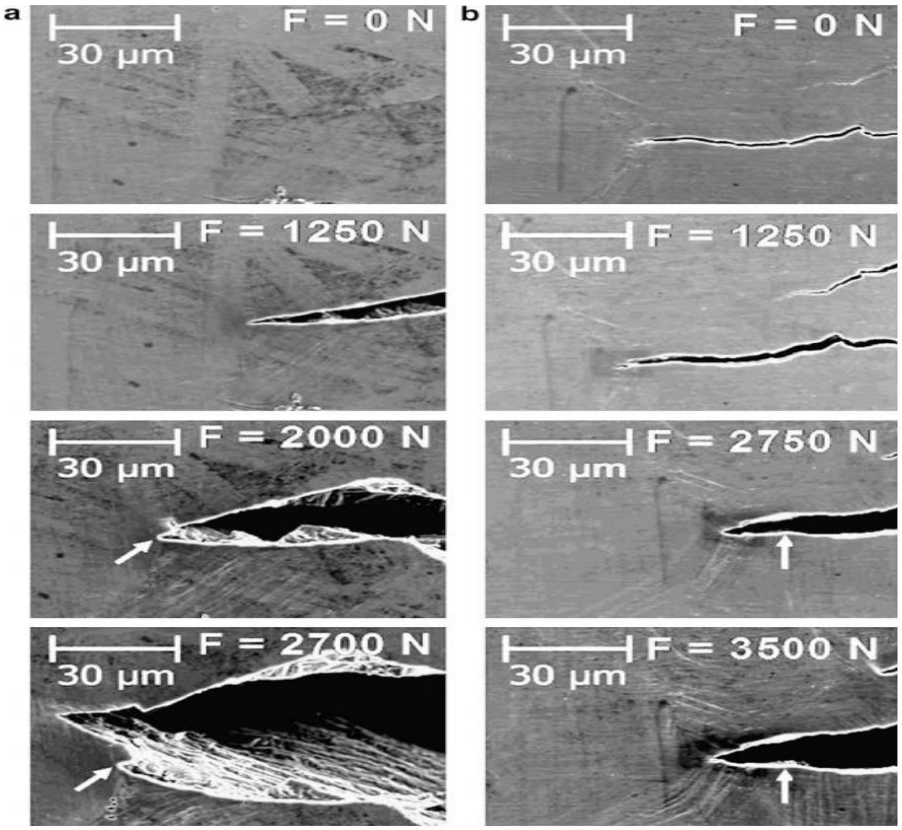

FIGURE 5. Scanning electron micrographs of (a) martensitic (a/W = 0.513) and (b) pseudoelastic (a/W = 0.506) NiTi SMAs at applied loads of 0, 1250, 2000 and 2700 N and 0, 1250, 2750 and 3500 N, respectively, during an in situ fracture experiment [26]

The results in this study show that a NiTi SMA with 50.7 at.% Ni shows a lower resistance to crack propagation when martensite forms in front of the crack tip prior to crack propagation as compared to the case where cracks grow into austenite without martensite at the crack tip. [26]. Stress-strain characteristics of NiTi specimen: Nanoindnetation technique is used to estimate mechanical properties including the measurement of elastic modulus, hardness, fracture toughness, residual stresses, creep and stress-strain relationship. The following study is concentrated on deriving stress-strain curve by nano-indentation using spherical indenter tips with varying R (radius of indentor) as well as with a Berkovich indentor. The significant difference in indentation height (h) with i. incremental applied load and ii. varying tip bluntness at the same load P is given. Fig.6 shows the increment in h_{max} (~320%) with seven-fold increase in the load P. Interestingly, increment in h_{max} with P_{max} is almost 1.5 times higher in the case of nanoindentation of NiTi alloy with a spherical tip compared to a Berkovich tip.

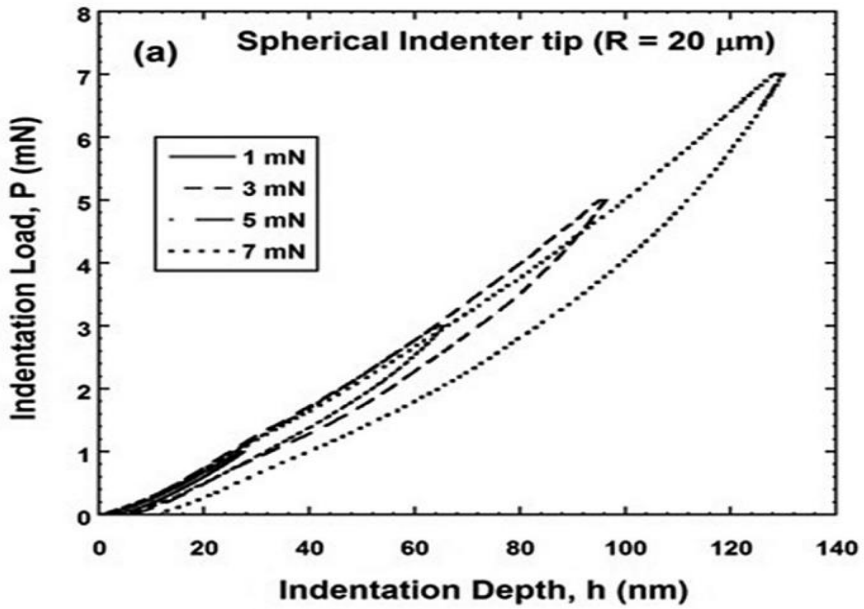

FIGURE 6. Indentation depth (h) vs the indentation load (p) [27]

Now, P-h curve obtained upon indenting the specimen with P_{max}~5mN using both Berkovich and varying indentor tips is given in Fig.7. Close scrutiny gave the conclusion that h_{max} values reduce significantly upon indenting NiTi with increasingly blunt spherical tips in comparison to a Berkovich tip at a particular constant value of P_{max}. The sharpest Berkovich tip (R ~ 100 nm) penetrates till h_{max} of ~ 250 nm (P_{max} ~ 5 mN). However, h_{max} decrease to ~ 150 nm, 100 nm and 40 nm as R increases to 10 μm, 20 μm and 50 μm respectively.

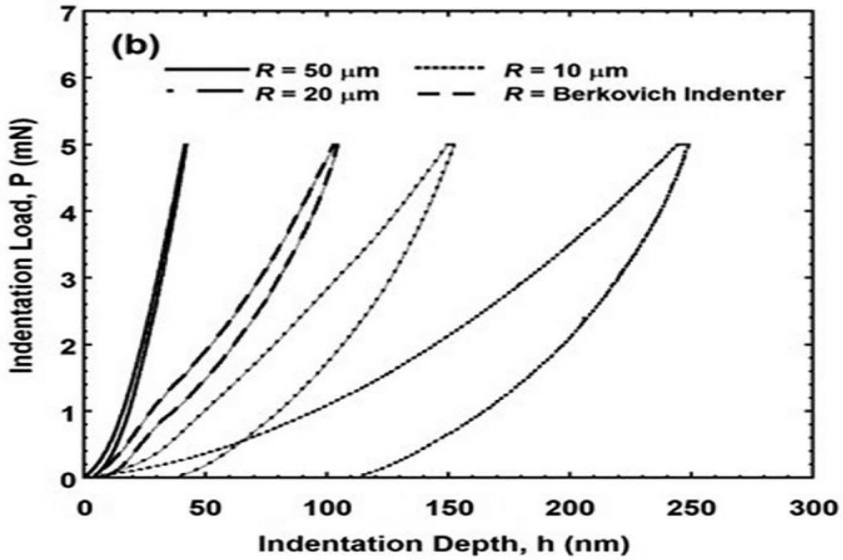

FIGURE 7. Indentation load (P) vs indentation depth (h) using Berkovich and varying indentor tips [27]

where stress (indentation) is given by $\sigma_{ind-S} = P/\pi a^2$; where P is the load (in Newton) and a is the contact radius and the corresponding strain (ε_{ind-S}) can be calculated by modified Hertz's relation $\sigma_{ind-S} = E_{eff} * \varepsilon_{ind-S}$; E_{eff} ……(2) is the effective modulus between the NiTi specimen and indenter [27].

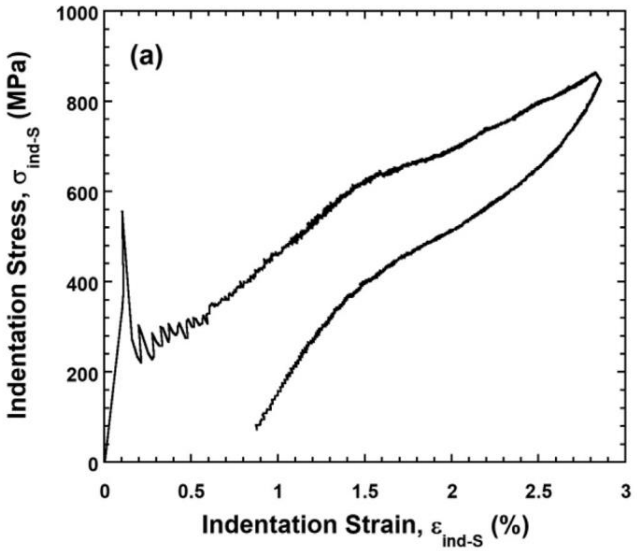

FIGURE 8. Indentation stress vs strain curve [27]

Now, to further give data about the stress-strain relationship of NiTi shape memory alloy specimens, behaviours of as-cast (AC), hot rotary swaged (HS), and hot-rolled (HR) NiTi materials under superelastic tensile loading are studied (shown in Fig.9). Strain level is defined by ΔL/L, where ΔL refers to the extension measured by the extensometer and L is the original length of the sample. Although the strain level at which major phase transformation activity was triggered was almost the same value at around 0.3−0.4% for all three materials, the stress level shows a major difference: HS NiTi has the largest phase transformation stress of nearly 200 MPa, followed by AC NiTi at ~150 MPa, and HR NiTi is merely ~110 MPa. [20]

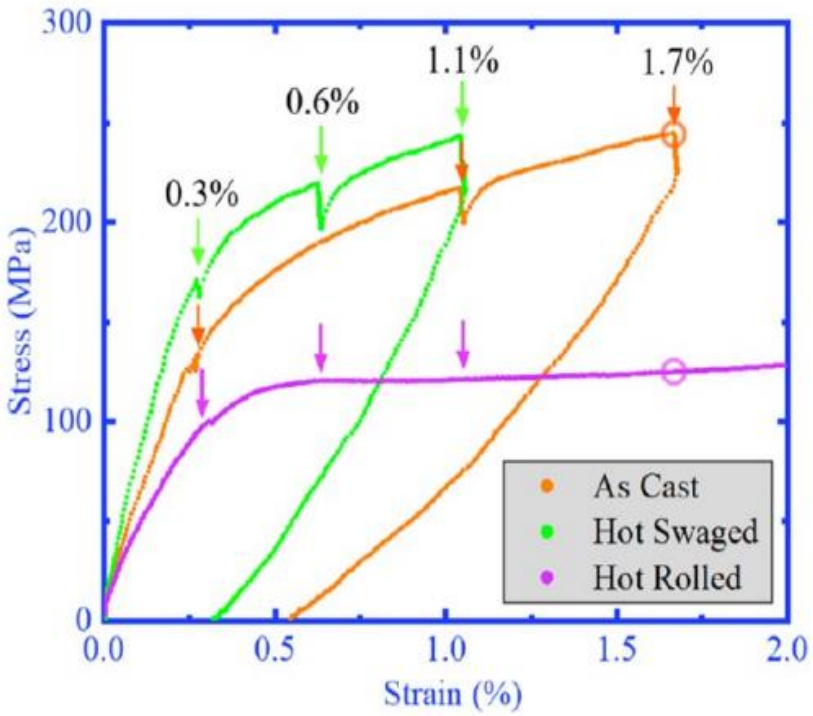

FIGURE 9. Stress vs Strain curve of AS, HS and HR NiTi specimens [20]

The tensile stress-strain responses of as-deposited specimens at z-heights of 1.5 mm (sample 1), 5.5 mm (sample 2) and 11.5 mm (sample 3) are shown in Fig. 10. The mechanical properties including the critical stress that induced transformation from austenite to martensite (c), was illustrated by the tangent method.

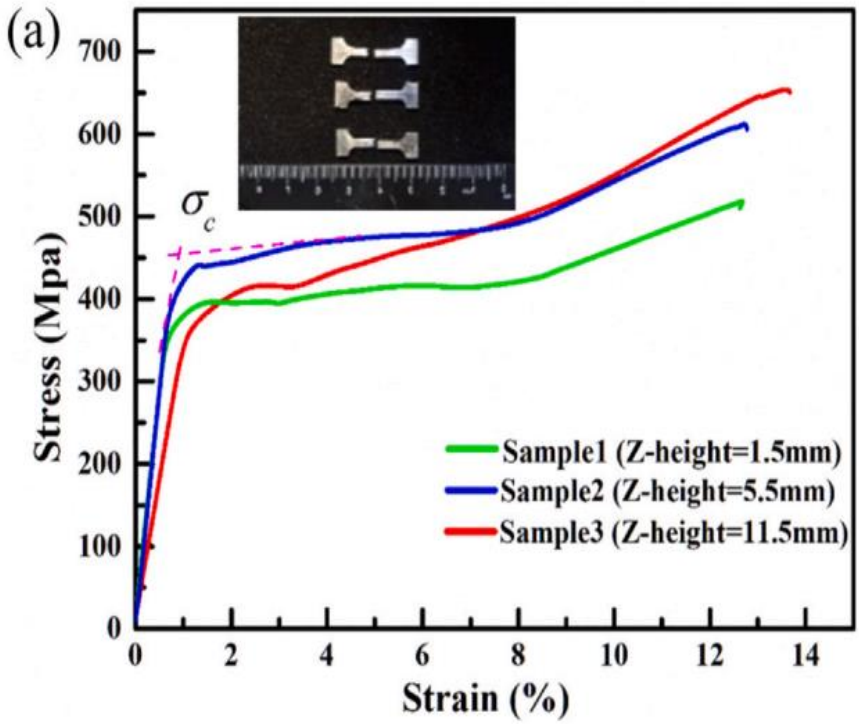

FIGURE 10. Stress-strain tensile curves of three samples at different height z [28]

All these samples show typical super elasticity characteristics at room temperature. Firstly, the stress increased with the increase of strain, and the elastic deformation of austenite occurred. Then, the stress-induced martensitic transformation began when the applied stress exceeded the critical stress, which is usually accompanied by plastic deformation. Subsequently, the residual austenite experienced three phases of stress-induced martensitic transformation, reorientation and plastic deformation until it fractured. [28] Yield and ultimate strength: Yield strength is the amount of maximum stress that can be developed without causing any plastic deformation and ultimate tensile strength or ultimate strength is the maximum stress that a material

can withstand without rupture. Now, yield strength of NiTi varies from 70-140MPa (in Martensitic phase) or 195-690MPa (in austenitic phase); while ultimate strength can vary from 754-960MPa depends on Ni/Ti ratio, mechanical working and heat treatment. Table 2 shows the mechanical properties of as-rolled $Ni_{50}Ti_{50}$ specimen, especially ultimate tensile and yield strength, as a result of tensile tests which were conducted at a temperature 15°C lower than M_s (Martensite starting temperature). [29].

Table 2. To show the characteristic temperatures

Specimen	**M_s (°C)**	**A_s(°C)**	**Yield strength (MPa)**	**Ultimate tensile strength (MPa)**
$Ni_{50}Ti_{50}$	58	88	192	801

Table 2. To show the characteristic temperatures {i.e. Martensite (M_s) and Austenite (A_s) starting temperatures} and yield and ultimate tensile strengths of $Ni_{50}Ti_{50}$ sample [29] The corresponding mechanical properties, including yield stress (σ_S), fracture strain (ε_F), critical stress of stress-induced martensite (SIM) (σ_{SIM}) of solution treated and three samples of annealed NiTi samples was compared in Table 3 and it was found that the annealed NiTi samples possess much higher yield stress than the solution-treated one. Even the minimum yield stress of the annealed NiTi samples is more than two times larger than that of solution-treated one. [30].

TABLE 3. yield stress (σS), fracture strain (εF), critical stress of SIM (σSIM) of solution treated and annealed NiTi samples.

NiTi sample	**σ_S(MPa)**	**ε_F(%)**	**σ_{SIM}(MPa)**
Solution-treated	923.1	41.1	342.1
Annealed for 4h	2552.1	11.7	267.8
Annealed for 8h	2314.3	13.5	216.6
Annealed for 12h	2211.2	14.6	160.2

4. Uses of NiTi based shape memory alloys in manufacturing of spring tyre for Mars Rover

To this day, all the rovers deployed for surface exploration on mars, from Sojourner to Curiosity, have had aluminium wheels. Curiosity weighed about 1000kgs, much more than its predecessors, with a wheel diameter of 0.5m and wheels thickness of just 0.75mm. In addition to this, there were skin grousers (treads) made of titanium provided for better traction. As of 2013, engineers at Jet Propulsion Laboratory discovered a lot more damage of the wheels than expected. This triggered redesign of wheels for future Mars surface exploration missions. [31] During the mid-2000s, NASA Glenn engineer Vivake Asnani worked with industry partner Goodyear to develop the Spring Tire. When the spring tire was first introduced, it was made of coiled piano wire woven to form a mesh. But the problem faced with the material used was that it undergoes plastic deformation, which was undesirable for extensive missions. To solve this problem, binary NiTi (nitinol) based shape memory alloy wires were used for their superelasticity.
The first NASA vehicle to use wire mesh wheels was the Lunar Roving Vehicle (LRV). [32]

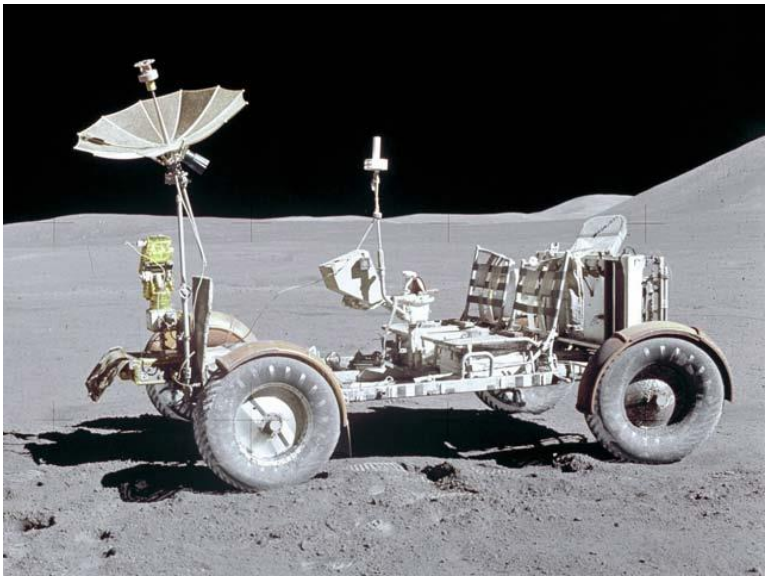

FIGURE 11. Lunar Roving Vehicle with four wire mesh wheels [32]

These glorified effects that memory alloys possess are originated through martensitic transformation (MT), as discussed before, and therefore, depending on the characteristics of the MT, i.e., transformation temperatures (TTs), transformation path, thermal and stress hysteresis (ΔTH and ΔσH, respectively), transformation strain, cycling stability, the field of SMA applications is determined. To alter the characteristics of memory alloys, methods of chemical alloying and the thermomechanical treatments are employed. [33]

5. Conclusion

In this present paper, we investigated and provided an overview of the characteristic physical properties of shape memory alloys where the shape memory effect (SME) and superelastic effect (SE) is explained. NiTi based shape memory alloy exhibit martensite phase at low temperatures and austenite temperature at higher temperatures. These effects are a result of thermo elastic martensitic phase transformations. A surge in mechanical properties and change in transformation behaviour was observed by researchers when a third (ternary) metal was added to NiTi alloy using suitable processing techniques. For advancement in application of NiTi based shape memory alloys, enhancement in its mechanical properties, such as Young's modulus, ultimate tensile strength, yield strength and hardness, by adding an equally strong metal to it .i.e. zirconium. It doesn't just limit to this, but successful improvement in ternary NiTi based shape memory alloy can be seen by adding fourth (quaternary) metal to it. New researches are concentrated on the behavioural characteristics, most importantly their mechanical properties, of ternary and quaternary NiTi based shape memory alloys such as Ni-Ti-W, Ti-Ni-Zr, etc.

Reference

[1]. Uddeshya Shukla, Kamal Garg, "Journey of smart material from composite to shape memory alloy (SMA), characterization and their applications", Smart Materials in Medicine 4 (2022) pp 227–242, https://doi.org/10.1016/j.smaim.2022.10.002

[2]. Jinguo Ge, Bo Yuan, Lun Zhao, Ming Yan, Wei Chen, Liang Zhang, "Effect of volume energy density on selective laser melting NiTi shape memory alloys: microstructural evolution, mechanical and functional properties", Journal of materials research and technology 2022 pp 2872-2888, https://doi.org/10.1016/j.jmrt.2022.08.062

[3]. Guangfeng Shi, Lunxiang Li, Zhenglei Yu, Pengwei Sha, Qing Cao, Zezhou Xu, Yuting Liu B, Yunting Guo, Jiashun Si, Jiabao, Liu e, "Effect of crystallographic anisotropy on phase transformation and tribological properties of Ni-rich NiTi shape memory alloy fabricated By LPBF", Optics& Laser Technology 157 (2022) 108731, https://doi.org/10.1016/j.optlastec.2022.108731

[4]. Kengfeng Xu, Jiao Luo, Cong Li, "Mechanisms of stress-induced martensitic transformation and transformation-induced plasticity in NiTi shape memory alloy related to superelastic stability", Scripta Materialia 217 (2022) 114775, https://doi.org/10.1016/j.scriptamat.2022.114775

[5]. Luc Saint-Sulpice, Vincent Legrand, Shabnam Arbab-Chirani, Sylvain Calloch, Cédric Doudard, "Fatigue life study of superelastic NiTi Shape Memory Alloys using Self-heating under cyclic loading method", International Journal of Fatigue 165 (2022) 107208, https://doi.org/10.1016/j.ijfatigue.2022.107208

[6]. Zhongyin Zhu, Shaohua Yan, Hui Chen, Guoqing Gou "Unprecedented combination of strength and ductility in laser welded NiCoCr medium entropy alloy Joints", Zhongyin ZhuShaohua YanHui ChenGuoqing Gou1–45567891011121314, https://doi.org/10.1016/j.msea.2020.140501

[7]. Himanshu Vashishtha , Jayant Jain, "Unraveling the passive film formation and degradation mechanism of NiTi shape memory alloy: An experimental investigation", Materials Today Communications 33 (2022) pp 104734, https://doi.org/10.1016/j.mtcomm.2022.104734

[8]. Guangfeng Shi , Lunxiang Li , Zhenglei Yu , Ruiyao Liu , Pengwei Sha , Zezhou Xu, Yunting Guo , Rui Xi, Jiabao Liu, Renlong Xin, Lixin Chen, Xiebin Wang, Zhihui Zhang, "The interaction effect of process parameters on the phase transformation behavior and tensile properties in additive manufacturing of Ni-rich NiTi alloy", Journal of Manufacturing Processes 77 (2022) pp539-555, https://doi.org/10.1016/j.jmapro.2022.03.027

[9]. Gaofeng Liu, Shihui Zhou, Pengyu Lin , Xuemei Zong, Zhikai Chen, Zhihui Zhang , Luquan Ren, "Analysis of microstructure, mechanical properties, and wear performance of NiTi alloy fabricated by cold metal transfer based wire arc additive manufacturing", Journal of Material Research and Technology (2022) ;20: pp246-259, https://doi.org/10.1016/j.jmrt.2022.07.068

[10]. Georgia Crowther, Dimitrios (Dimi) Apostolopoulos, Stuart Heys, "Tensegrital wheel for enhanced planetary surface mobility: Part 1 –design and evolution", Journal of Terramechanics 100 (2022) pp 11–24, https://doi.org/10.1016/j.jterra.2021.11.008

[11]. Jie Chen, Zengyong Wang, Shuang Wang, Zheng Xiang, Xianfeng Shen, Shuke Huang, Qin Yang, "Mechanical and functional properties of HfH2-decorated NiTi shape memory alloy fabricated by laser powder-bed fusion", Journal of Alloys and Compounds 913 (2022) 165296, https://doi.org/10.1016/j.jallcom.2022.165296

[12]. Brinda Bhattarai, Chetasvani Dutta, Shri Lakshmi K.M., Deeptha A.S., Kavya Nair, Dr. Aravind Seeni, "Design and Analysis of Lunar Rover Wheels using Finite Element Modelling", SPAST Abstracts (2021)

[13]. Xie Dong, Yu Fei , J.B. Wang, Y.Y. Su , F.J. Jing, Y.X. Leng , Nan Huang, " Deformation behavior of TiO2 films deposited on NiTi shape memory alloy after tensile and water-bath heating tests", https://doi.org/10.1016/j.surfcoat.2021.127151

[14]. Akhil Bhardwaj, Mihir Ojha, Ashutosh Garudapalli, Amit Kumar Gupta, "Microstructural, mechanical and strain hardening behaviour of NiTi alloy subjected to constrained groove pressing and ageing treatment", https://doi.org/10.1016/j.jmatprotec.2021.117132

[15]. Xiebin Wanga, Xiayang Yaoc , Dominique Schryvers, Bert Verlindend, Guilong Wanga , Guoqun Zhaoa , Jan Van Humbeeck, Sergey Kustov, "Anomalous stress-strain behavior of NiTi shape memory alloy close to the border of superelastic window", Scripta Materialia 204 (2021) 114135, https://doi.org/10.1016/j.scriptamat.2021.114135

[16]. K. Mehrabi, M. Brunckoa, A.C. Kneissl, "Microstructure, mechanical and functional properties of NiTi-based shape memory ribbons", Journal of Alloys and Compounds 526 (2012) pp 45–52, https://doi.org/10.1016/j.jallcom.2012.02.097

[17]. Sachin Oak, Vinod Belwanshi, Kedarnath Rane, Kiran Bhole, Bharatbhushan Kale, "Comparison of binary, ternary and quaternary shape memory alloys and techniques to enhance their mechanical properties: A focused review", Materials Today: Proceedings 68 (2022) 2199–2209, https://doi.org/10.1016/j.matpr.2022.08.433

[18]. LiqiangWang, CongWang, Lai-ChangZhang, LiangyuChen, Weijie Lu & Di Zhang, "Phase transformation and deformation behavior of NiTi-Nb eutectic joined NiTi wires" (2016)

[19]. Arthur Khismatullin, Oleg Panchenko, Dmitry Kurushkin, Ivan Kladov and Anatoly Popovich, "Functional and Mechanical Properties of As-Deposited and Heat Treated WAAM-Built NiTi Shape-Memory Alloy", metals 2022, 12(6), 1044, https://doi.org/10.3390/met12061044

[20]. Zifan Wang, Jingwei Chen, Radim Kocich, Samuel Tardif, Igor P. Dolbnya, Lenka Kuncická, Jean-Sébastien Micha, Konstantinos Liogas, Oxana V. Magdysyuk, Ivo Szurman, and Alexander M. Korsunsky, "Grain Structure Engineering of NiTi Shape Memory Alloys by Intensive Plastic Deformation", ACS Appl. Mater. Interfaces 2022, 14, 31396−31410, https://doi.org/10.1021/acsami.2c05939?urlappend=%3Fref%3DPDF&jav=VoR&rel=cite-as

[21]. https://link.springer.com/article/10.1007/s11837-021-04937-y/figures/1

[22]. Rodayna Hmede, Frédéric Chapelle and Yuri Lapusta, "Review of Neural Network Modeling of Shape Memory Alloys", https://www.mdpi.com/journal/sensors

[23]. Sachin Oak, Vinod Belwanshi, Kedarnath Rane, Kiran Bhole, Bharatbhushan Kale, "Comparison of binary, ternary and quaternary shape memory alloys and techniques to enhance their mechanical properties: A focused review", Materials Today: Proceedings 68 (2022) pp 2199–2209, https://doi.org/10.1016/j.matpr.2022.08.433

[24]. Inderjit Chopra and Jayant Sirohi, "Shape Memory Alloys (SMAs)", https://doi.org/10.1017/CBO9781139025164.004

[25]. Guotai Li, Tianyu Yu, Ning Zhang, Mingjun Chen, "The effect of Ni content on phase transformation behavior of NiTi alloys: An atomistic modeling study", Computational Materials Science 215 (2022) 111804, https://doi.org/10.1016/j.commatsci.2022.111804

[26]. S. Gollerthan, M.L. Young, A. Baruj, J. Frenzel, W.W. Schmahl, G. Eggeler, "Fracture mechanics and microstructure in NiTi shape memory alloys", Acta Materialia 57 (2009) pp 1015–1025, https://doi.org/10.1016/j.actamat.2008.10.055

[27]. Sujith Kumar S, I. Anand Kumar, Lakhindra Marandi, Indrani Sen, "Assessment of small-scale deformation characteristics and stress-strain behavior of NiTi based shape memory alloy using nanoindentation", Acta Materialia 201 (2020) 303–315, https://doi.org/10.1016/j.actamat.2020.09.080

[28]. Lin Yua, Keyu Chena, Yuanling Zhanga , Jie Liua, Lei Yangb, Yusheng Shi, "Microstructures and mechanical properties of NiTi shape memory alloys fabricated by wire arc additive manufacturing", Journal of Alloys and Compounds 892 (2021) 162193, https://doi.org/10.1016/j.jallcom.2021.162193

[29]. Zhen-zhen BAO, Shun GUO, Fu XIAO, Xin-qing ZHAO, "Development of NiTiNb in-situ composite with high damping capacity and high yield strength", Materials International 21(2011) pp 293-300, https://doi.org/10.1016/S1002-0071(12)60060-4

[30]. Bingyao Yan, Shuyong Jiang a, Dong Sun, Man Wang, Junbo Yu, Yanqiu Zhang, "Martensite twin formation and mechanical properties of B2 austenite NiTi shape memory alloy undergoing severe plastic deformation and subsequent annealing", Materials Characterization 178 (2021) 111273, https://doi.org/10.1016/j.matchar.2021.111273

[31]. Giovanni Zambelli Arsequell, "RESEARCH OF SHAPE MEMORY ALLOY WHEELS FOR MARS ROVERS", Tampere University of Applied Sciences, https://www.theseus.fi/bitstream/handle/10024/503368/Zambelli_Giovanni.pdf?sequence=3&isAllowed=y

[32]. https://www.nasa.gov/specials/wheels/

[33]. Woo-Chul Kim, Ka-Ram Lim, Won-Tae Kim, Eun-Soo Park, Do-Hyang Kim, "Recent advances in multicomponent NiTi-based shape memory alloy using metallic glass as a precursor", https://doi.org/10.1016/j.pmatsci.2021.100855